Journal of Intelligent & Robotic Systems (2024) 110:39
https://doi.org/10.1007/s10846-023-01967-3

REGULAR PAPER

A Switched Control Strategy for Avoiding Flip Ambiguities in 3D Formations

Farid Sahebsara [1] · **Marcio de Queiroz**[1]

Received: 22 November 2022 / Accepted: 11 September 2023 / Published online: 23 February 2024

Abstract
Flip ambiguities are a notorious issue with distance-based formation control due to the presence of unwanted equilibrium points in the formation dynamics. We propose a switched control system for preventing these ambiguities in 3D formations composed of tetrahedra. The approach contains a switching strategy that steers the formation of mobile robots towards the desired configuration for all initial positions, excluding certain collocated, collinear, or coplanar cases, by applying the standard distance-based controller and/or rigid-body maneuvers to subformations. Simulations demonstrate that the proposed formation control system can lead to faster formation acquisition and less control effort than an existing method.

Keywords Multi-agent systems · Formation control · Nonlinear Control

1 Introduction

A basic problem in the field of formation control is for a team of mobile robots to maintain a desired configuration in space [4, 15]. This requirement is intrinsic to tasks such as patrolling, monitoring, surveying, and element tracking over large geographical areas, and co-transporting large, heavy objects. One solution to this problem is regulating a group of inter-robot distances encoded by the prescribed configuration [4, 10]. The advantage of this approach, commonly called distance-based formation control (DBFC) [16], is its ability to be implemented in a distributed fashion. Unfortunately, there may not be a one-to-one relationship between the desired spatial configuration and the set of inter-robot distances, leading to the system possibly converging to an incorrect formation. This manifests itself mathematically as multiple equilibrium points for the distance dynamics of the multi-robot system. One is then left with the challenge of avoiding the undesired equilibria and steering the robots toward the equilibrium point associated with the desired formation shape.

✉ Marcio de Queiroz
mdeque1@lsu.edu

Farid Sahebsara
fsaheb1@lsu.edu

[1] Department of Mechanical & Industrial Enginering, Louisiana State University, Baton Rouge, LA 70803, USA

The issue mentioned above is partly resolved by imposing a sufficient number of controlled distances so that the formation graph becomes *rigid* [1, 4]. Graph rigidity reduces the undesired equilibria to formations that are flipped or reflected variants of the desired shape. In this situation, the convergence to a formation that is isomorphic to the desired formation or to a flipped/reflected one is dependent on the agents' initial positions. That is, DBFC utilizing rigid graphs only ensures local stability.

Recently, a few methods have been proposed to handle the local stability nature of rigid DBFC. This was achieved by introducing another controlled variable that discerns the desired formation from an ambiguous one. For instance, [5, 12, 17] increased the region of attraction to the desired planar formation by utilizing distance and angle-type constraints. In [2], the signed area of a triangle was employed as the other controlled variable. This idea was later generalized in [11] to triangulated 2D formations. Other results based on the signed area approach can be found in [3, 19] . For 3D formations, [6] applied constraints to the signed volume of a tetrahedron. The results discussed above all necessitate conditions on the number of agents, control parameters, and/or the triangulations or tetrahedralizations of the desired formation. A method named the orthogonal basis approach avoided these restrictions by projecting the states and control inputs onto orthogonal spaces [13, 14].

In this paper, we reexamine the original challenge posed above. Specifically, the contribution of this paper is a solution

for avoiding flip ambiguities that does not utilize additional controlled variables and is founded mainly on the conventional DBFC of [10] for 3D formations. Furthermore, our solution ensures attraction to the desired shape for any initial condition excluding certain collocated, collinear, and coplanar cases. We consider here that the topology of the desired and actual formations are based on the type I Henneberg insertion for 3D graphs [7] which starts with three connected vertices and is grown by adding a vertex and three edges to the graph. The rigidity of the graph remains intact with these insertions since the graph is formed by tetrahedra (i.e., triangular pyramids). We propose a control system that includes a switching strategy based on characterizations of the region of attraction to the desired formation and to the flip-ambiguous formation. In particular, we formulate a metric for determining in what region of attraction a robot is present at all times. This determines if DBFC is applied or if subformations need to be maneuvered as a virtual rigid body to relocate the robot in the desired region of attraction. The control scheme is illustrated via computer simulations and compared with the orthogonal basis control of [14]. An early version of this paper was published in [18] where the formation controller was applied to sequentially-grown 2D formations by employing triangulations in the formation graph. In comparison to [18], the present result considers the more complicated 3D case and includes a proof of stability for the controller.

Notation In the following, $\|\cdot\|$ denotes the Euclidean norm of a vector, $|\cdot|$ is the cardinality of a set, and $\text{proj}_u v := \frac{v \cdot u}{\|u\|^2} u$ denotes the projection of vector v onto vector u.

2 Graph Theory

An undirected graph G is described by the pair $(\mathcal{V}, \mathcal{E})$, where $\mathcal{V} = \{1, 2, \ldots, N\}$ is the set of vertices and $\mathcal{E} = \{(i, j) | \, i, j \in \mathcal{V}, i \neq j\} \subset \mathcal{V} \times \mathcal{V}$ is the set of undirected edges. The set of neighbors of vertex $i \in \mathcal{V}$ is given by $\mathcal{N}_i(\mathcal{E}) = \{j \in \mathcal{V} | (i, j) \in \mathcal{E}\}$. If $q_i \in \mathbb{R}^3$ is the coordinate of vertex i of a 3D graph, then a framework F is the pair (G, q) where $q = [q_1, \ldots, q_N] \in \mathbb{R}^{3N}$.

Let $\mathcal{T} : \mathbb{R}^3 \to \mathbb{R}^3$ be such that $\mathcal{T}(x) = Qx + d$ where $Q \in SO(3)$ and $d \in \mathbb{R}^3$. Framework $F = (G, q)$ is rigid in $\mathbb{R}^3$ if all of its continuous motions satisfy $q_i(t) = \mathcal{T}(q_i)$ for $i = 1, \ldots, N$ and $\forall t \geq 0$ [8]. A 3D rigid framework is minimally rigid if and only if $|\mathcal{E}| = 3N - 6$ [4]. The edge function of a minimally rigid framework $\gamma : \mathbb{R}^{3N} \to \mathbb{R}^{3N-6}$ is defined as

$$\gamma(q) = \left[\ldots, \left\|q_i - q_j\right\|^2, \ldots\right], \quad (i, j) \in \mathcal{E}. \tag{1}$$

The rigidity matrix $R : \mathbb{R}^{3N} \to \mathbb{R}^{|\mathcal{E}| \times 3N}$ is defined as

$$R(q) = \frac{1}{2} \frac{\partial \gamma(q)}{\partial q} \tag{2}$$

where $\text{rank}[R(q)] \leq 3n - 6$ [4]. A 3D framework is said to be infinitesimally rigid if and only if $rank\,[R(q)] = 3N - 6$ in $\mathbb{R}^3$ [4]. Frameworks (G, q) and $(G, \hat{q})$ are equivalent if $\gamma(q) = \gamma(\hat{q})$, and are congruent if $\left\|q_i - q_j\right\| = \left\|\hat{q}_i - \hat{q}_j\right\|$ for *all* distinct vertices i and j in $\mathcal{V}$ [9]. If infinitesimally rigid frameworks (G, q) and $(G, \hat{q})$ are equivalent but not congruent, they are flip- or flex-ambiguous [4]. In this paper, we focus on flip ambiguities (see Fig. 1 for an example) because flex ambiguities result from a momentary loss of graph edges, which we consider cannot happen here.

A 3D minimally rigid framework can be built using the type I Henneberg insertion in 3D [7]. Beginning with triangular framework, this technique grows the graph by the successive addition of a vertex with three undirected edges, leading to a tetrahedralized, polyhedron framework. Hereafter, such a framework is called a 3D Henneberg framework.

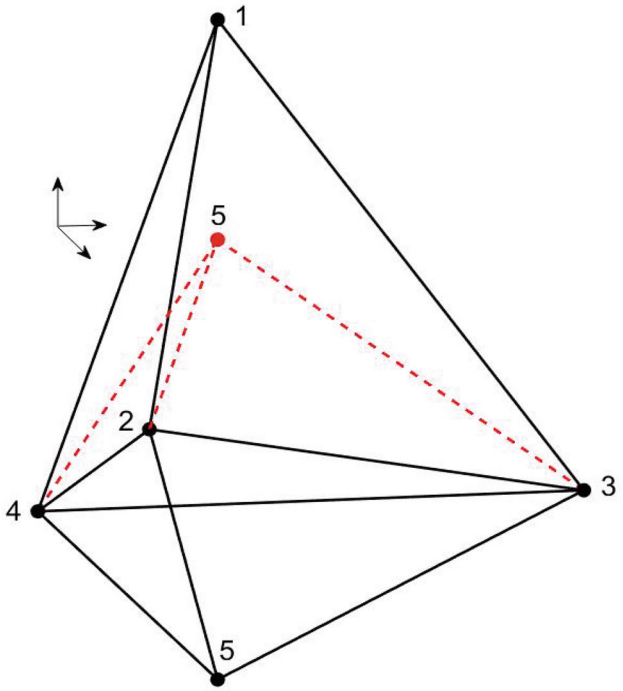

Fig. 1 Flip ambiguity in 3D: edges (2,5), (3,5), and (4,5) are reflected about the plane formed by vertices 2, 3, and 4 producing equivalent frameworks. Note that the frameworks are not congruent since distance $\|q_1 - q_5\|$ is not the same in the two frameworks

3 Problem Statement

We consider an N-robot system where $N \geq 4$ that needs to acquire a 3D formation encoded by $3N-6$ desired distances d_{ij}. The desired formation is modeled by framework $F^* = (G, \mathbf{q}^*)$ where $G = (\mathcal{V}, \mathcal{E})$, $|\mathcal{V}| = N$, $|\mathcal{E}| = 3N-6$, $\left\|q_i^* - q_j^*\right\| = d_{ij}$, $(i,j) \in \mathcal{E}$ with $q_i^* \in \mathbb{R}^3$, and $\mathbf{q}^* = \left[q_1^*, ..., q_N^*\right]$. The following assumptions are made regarding the desired framework:

A1. F^* is a 3D Henneberg framework with edge set $\mathcal{E} = \{(1,2),(1,3),(2,3),(1,4),(2,4),(3,4),\ldots,(k-3,k),(k-2,k),(k-1,k),\ldots,(N-3,N),(N-2,N),(N-1,N)\}$. [1]

A2. F^* is known to all robots beforehand.

The robot system is represented by $F(t) = (G, \mathbf{q}(t))$ where $\mathbf{q} = \left[q_1, ..., q_N\right]$ and $q_i \in \mathbb{R}^3$ is the ith robot position. Edge $(i,j) \in \mathcal{E}$ in F indicates that robots i and j can both measure their relative position and can communicate with each other to exchange information. We assume each robot is governed by the following equation of motion

$$\dot{q}_i = u_i, \quad \forall i \in \mathcal{V} \tag{3}$$

where $u_i \in \mathbb{R}^3$ is the control input. We use the notation $F_k(t) = (G_k, \mathbf{q}_k(t)) \subseteq F(t)$, where $G_k = (\mathcal{V}_k, \mathcal{E}_k)$, $\mathcal{V}_k = \{1,\ldots,k\}$, $\mathcal{E}_k \subseteq \mathcal{E}$, $\mathbf{q}_k = \left[q_1, ..., q_k\right]$, and $k < N$, to denote subformation k. A similar notation is used for subformations of F^*.

The objective is to synthesize a control scheme that avoids flip ambiguities by only utilizing distance constraints. That is, we do not enforce other constraints (e.g., the signed volume) on the 3D formation.

4 Flip Ambiguity

To demonstrate how flip ambiguities can occur in the given problem, let us consider the conventional DBFC [4, 10]. Define the relative position of two robots as $q_{ij} = q_i - q_j$ and the corresponding distance error-like variable as

$$s_{ij} = \left\|q_{ij}\right\|^2 - d_{ij}^2, \ \forall (i,j) \in \mathcal{E}. \tag{4}$$

Consider the Lyapunov function candidate

$$W = \frac{1}{4}\sum_{(i,j)\in\mathcal{E}} s_{ij}^2 = \frac{1}{4} s^\mathsf{T} s \tag{5}$$

where $s = [s_{12}, \ldots, s_{(N-1)N}] \in \mathbb{R}^{|\mathcal{E}|}$ is the vector of all the s_{ij}'s. The time derivative of Eq. (5) is given by

$$\dot{W} = \sum_{(i,j)\in\mathcal{E}} s_{ij} q_{ij}^\mathsf{T} \left(u_i - u_j\right). \tag{6}$$

where Eq. (3) was used. From the form of Eq. (6), the conventional DBFC is designed as [4, 10]

$$u_i = -\alpha \sum_{j\in\mathcal{N}_i(\mathcal{E})} q_{ij} s_{ij}, \ \forall i \in \mathcal{V} \tag{7}$$

where $\alpha > 0$ is a control gain. After substituting Eq. (7) into Eq. (6) and applying Eq. (2), we get [4]

$$\dot{W} = -\alpha s^\mathsf{T} R(q)\, R^\mathsf{T}(q)\, s \leq -\alpha \lambda_{\min}\left(RR^\mathsf{T}\right) s^\mathsf{T} s \tag{8}$$

where $\lambda_{\min}(\cdot)$ is the minimum eigenvalue. It can be shown that since $\lambda_{\min}(RR^\mathsf{T})$ is positive for sufficiently small initial errors, $s(0)$, then R is full row rank for all time and RR^T is positive definite [4]. Therefore, we conclude that $s = 0$ is locally exponentially stable from E qs. (5) and (8), which means the formation converges to the desired formation or to its flip-ambiguous version. That is, if we let $\mathbf{q}^*$ and $\mathbf{q}^{*a}$ be the equilibrium points of the desired and flip-ambiguous formations, respectively, then $F(t) \to F^*(\mathbf{q}^*)$ or $F(t) \to F^*(\mathbf{q}^{*a})$ as $t \to \infty$.

To determine if F will approach $F^*(\mathbf{q}^*)$ or $F^*(\mathbf{q}^{*a})$, consider that robots $1, \ldots, k-1$ have formed the desired shape and robot k is a new approaching robot that may create a flip ambiguity. In this case, Eq. (8) will simplify to

$$\dot{W} \leq -\alpha \lambda_{\min}\left(RR^T\right)\left[\left(\left\|q_{(k-3)k}\right\|^2 - d_{(k-3)k}^2\right)^2 + \left(\left\|q_{(k-2)k}\right\|^2 - d_{(k-2)k}^2\right)^2 + \left(\left\|q_{(k-1)k}\right\|^2 - d_{(k-1)k}^2\right)^2\right] \tag{9}$$

where the terms that meet the desired distance are zero, including $s_{(k-2)(k-1)}$, $s_{(k-3)(k-1)}$, and $s_{(k-3)(k-2)}$. Note that Eq. (9) is related to three edges of the tetrahedron composed by robots $k-3$, $k-2$, $k-1$, and k. Also, $\dot{W} = 0$ only when $\left\|q_{(k-3)k}\right\| = d_{(k-3)k}$, $\left\|q_{(k-2)k}\right\| = d_{(k-2)k}$, and $\left\|q_{(k-1)k}\right\| = d_{(k-1)k}$ which can be accomplished at $F_k^*(\mathbf{q}_k^*)$ or $F_k^*(\mathbf{q}_k^{*a})$. We can now state the following conjecture.

Conjecture: The region of attraction (RoA) to either equilibrium point is on the corresponding side of the plane containing q_{k-3}, q_{k-2}, and q_{k-1}; see Fig. 2.

This conjecture can be demonstrated by considering a formation with $N = 5$ for example where the desired formation is two back-to-back regular tetrahedra (triangular bipyramid) and robots 1-4 have already formed one half of the triangular bipyramid. The left panel of Fig. 3 shows robot 5 initially in the RoA to $F^*(\mathbf{q}^*)$. As a result, $F(t) \to F^*(\mathbf{q}^*)$ as $t \to \infty$ as we can see from the right panel of Fig. 3. In the left panel of Fig. 4, robot 5 is initially in the RoA to $F^*(\mathbf{q}^{*a})$ and outside

[1] This way of constructing the edge set leads to $|\mathcal{E}| = 3N-6$.

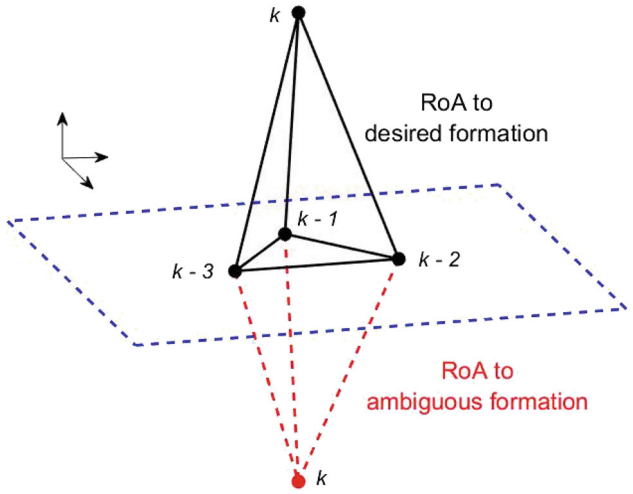

Fig. 2 Regions of attraction to $F_k^*(\mathbf{q}_k^*)$ and $F_k^*(\mathbf{q}_k^{*a})$

of the tetrahedron formed by robots 1-4. Now, the formation converges to $F^*(\mathbf{q}^{*a})$ instead (see Fig. 4 right panel). Lastly, Fig. 5 depicts a variation of the second case where robot 5 is initially positioned within the tetrahedron and near the borderline of the two RoAs. Again, the formation is attracted to $F^*(\mathbf{q}^{*a})$. In the following, we design a switched control scheme to prevent robots from converging to a flip ambiguity despite robot k being initially in the RoA to $F_k^*(\mathbf{q}_k^{*a})$.

5 Switched Control System

In this section, we present a switching control logic which when paired with the DBFC of Eq. (7) and certain rigid-body-like maneuvers avoids flip ambiguities. Therefore, the stability region of the closed-loop system is enlarged relative to the use of DBFC alone. Next, we explain the reasoning behind the proposed control system.

Let the RoA to $F_k^*(\mathbf{q}_k^*)$ and $F_k^*(\mathbf{q}_k^{*a})$ be represented by $\mathcal{R}(\mathbf{q}_k^*)$ and $\mathcal{R}(\mathbf{q}_k^{*a})$, respectively. The control system involves robots $k = 4, \ldots, N$ continuously checking if they are located in $\mathcal{R}(\mathbf{q}_k^*)$ or $\mathcal{R}(\mathbf{q}_k^{*a})$. If $q_k \in \mathcal{R}(\mathbf{q}_k^*)$, robot k simply employs the conventional DBFC. If $q_k \in \mathcal{R}(\mathbf{q}_k^{*a})$, then a maneuver is introduced in the formation to force robot k towards $\mathcal{R}(\mathbf{q}_k^*)$. The type of maneuver is dependent on where robot k is located in $\mathcal{R}(\mathbf{q}_k^{*a})$. Specifically, let the convex hull of $\mathbf{q}_l^*$ (i.e., the desired position of robots $1, \ldots, l$) be denoted by $\mathcal{C}(\mathbf{q}_l^*)$. If robot k satisfies the condition $q_k \in \mathcal{R}(\mathbf{q}_k^{*a}) \cap \mathcal{C}(\mathbf{q}_{k-1}^*)$, then it should translate towards the plane formed by robots $k-3$, $k-2$, and $k-1$ (the specific direction of translation will be given later) while F_{k-1} remains stationary until $q_k \in \mathcal{R}(\mathbf{q}_k^*)$. If $q_k \in \mathcal{R}(\mathbf{q}_k^{*a}) \cap \bar{\mathcal{C}}(\mathbf{q}_{k-1}^*)$ where $\bar{\mathcal{C}}(\cdot)$ is the complement of the convex hull, then F_{k-1} should undergo a rigid body rotation about a vector on the plane formed by robots $k-3$, $k-2$, and $k-1$ (the vector calculation will be specified later) while robot k remains stationary until $q_k \in \mathcal{R}(\mathbf{q}_k^*)$. An implicit condition for these maneuvers to be triggered is that subformation $F_{k-1}(t)$ has successively converged to $F_{k-1}^*(\mathbf{q}_{k-1}^*)$ because then there exists a boundary plane between $\mathcal{R}(\mathbf{q}_k^*)$ and $\mathcal{R}(\mathbf{q}_k^{*a})$ (see Fig. 2). Thus, if more than one robot, e.g. robots l and m where $l < m$, are in the RoA to their respective ambiguous equilibrium point, then the necessary maneuver is applied to robot l first and, once $q_l \in \mathcal{R}(\mathbf{q}_l^*)$, the necessary maneuver is applied to robot m. That is, the logic is applied sequentially to all robots who

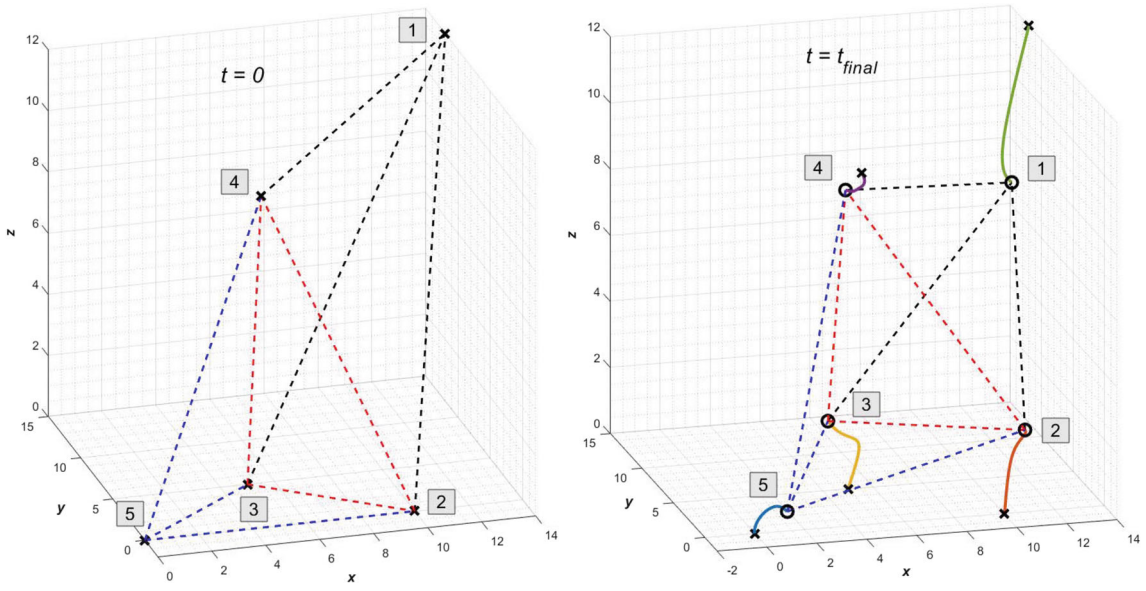

Fig. 3 Robot 5 initialized in the RoA to $F^*(\mathbf{q}^*)$. Crosses and circles denote initial and final positions, respectively

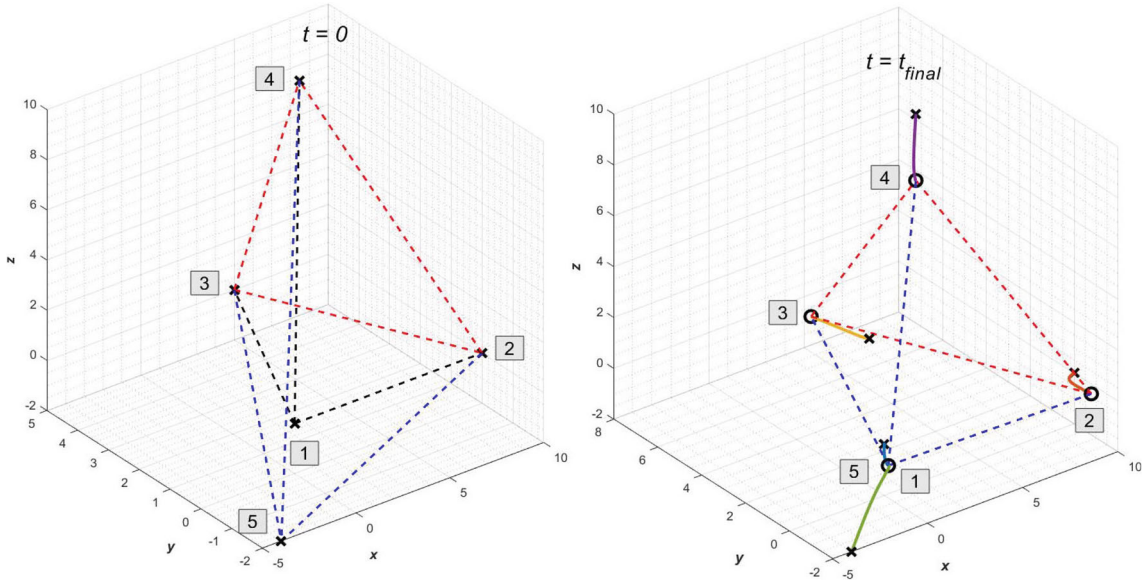

Fig. 4 Robot 5 initialized in the RoA to $F^*(\mathbf{q}^{*a})$ and *outside* of the tetrahedron formed by robots 1-4. Crosses and circles denote initial and final positions, respectively. Robots 1 and 5 ocupy same final position due to convergence to the ambiguous formation.

are located in $\mathcal{R}(\mathbf{q}_k^{*a})$. A summary of the algorithm is shown below.

Algorithm 1 Control Logic

repeat
  for Subformation $F_k^*(\mathbf{q}_k^*)$, $k = 4, ..., N$ **do**
    if Subformation $F_{k-1}^*(\mathbf{q}_{k-1}^*)$ is already acquired *[Eq. (17)]* **then**
      if $q_k \in \mathcal{R}(\mathbf{q}_k^{*a}) \cap \mathcal{C}(\mathbf{q}_{k-1}^*)$ **then**
        Translate robot k towards $\mathcal{R}(\mathbf{q}_k^*)$ *[2nd row of Eq. (15)]*
        Keep robots $k-1$ and $k-2$ stationary *[2nd row of Eq. (14)]*
        Apply DBFC to all other robots *[Eq. (13)]*
      else if $q_k \in \mathcal{R}(\mathbf{q}_k^{*a}) \cap \bar{\mathcal{C}}(\mathbf{q}_{k-1}^*)$ **then**
        Keep robot k stationary *[3rd row of Eq. (15)]*
        Rotate F_{k-1} to locate robot k in $\mathcal{R}(\mathbf{q}_k^*)$ *[3rd row of Eq. (14)]*
        Apply DBFC to all other robots *[Eq. (13)]*
      else
        Apply DBFC to all robots *[Eq. (13) and 1st row of Eqs. (14) and (15)]*
      end if
    else
      Apply DBFC to all robots *[Eq. (13) and 1st row of Eqs. (14) and (15)]*
    end if
  end for
until F^* is acquired

In order to mathematically formalize the algorithm, a few variables need to be introduced. Let c be the position of robot k relative to the centroid of the triangle composed of robots $k-3$, $k-2$, and $k-1$ (Fig. 6). Since we desire to calculate c from data local to the robots, we use the following formulas

$$c = \begin{cases} q_{k(k-3)} - \dfrac{q_{(k-1)(k-3)} + q_{(k-2)(k-3)}}{3}, & \text{for robot } k-3 \\ q_{k(k-2)} - \dfrac{q_{(k-1)(k-2)} + q_{(k-3)(k-2)}}{3}, & \text{for robot } k-2. \\ q_{k(k-1)} - \dfrac{q_{(k-3)(k-1)} + q_{(k-2)(k-1)}}{3}, & \text{for robot } k-1 \\ -\dfrac{q_{(k-3)(k)} + q_{(k-2)(k)} + q_{(k-1)(k)}}{3}, & \text{for robot } k. \end{cases} \tag{10}$$

If we let $\mathcal{Z}$ denote the plane formed by robots $k-3$, $k-2$, and $k-1$, the vector $p \in \mathcal{Z}$ perpendicular to vector $q_{(k-2)(k-1)}$ (see Figure 6) is defined by

$$p = \begin{cases} q_{(k-3)(k-2)} - \text{proj}_{q_{(k-1)(k-2)}} q_{(k-3)(k-2)}, & \text{for robot } k-2 \\ q_{(k-3)(k-1)} - \text{proj}_{q_{(k-2)(k-1)}} q_{(k-3)(k-1)}, & \text{for robot } k-1 \end{cases} \tag{11}$$

where the first (resp., second) equation is utilized by robot $k-2$ (resp., $k-1$). The vector normal to plane $\mathcal{Z}$ (see Fig. 6) is defined by

$$n = \begin{cases} q_{(k-1)(k-3)} \times q_{(k-2)(k-3)}, & \text{for robot } k-3; \\ q_{(k-3)(k-2)} \times q_{(k-1)(k-2)}, & \text{for robot } k-2; \\ q_{(k-2)(k-1)} \times q_{(k-3)(k-1)}, & \text{for robot } k-1 \end{cases} \tag{12}$$

where the first, second, and third equations are used by robots $k-3$, $k-2$, and $k-1$, respectively. This vector will help

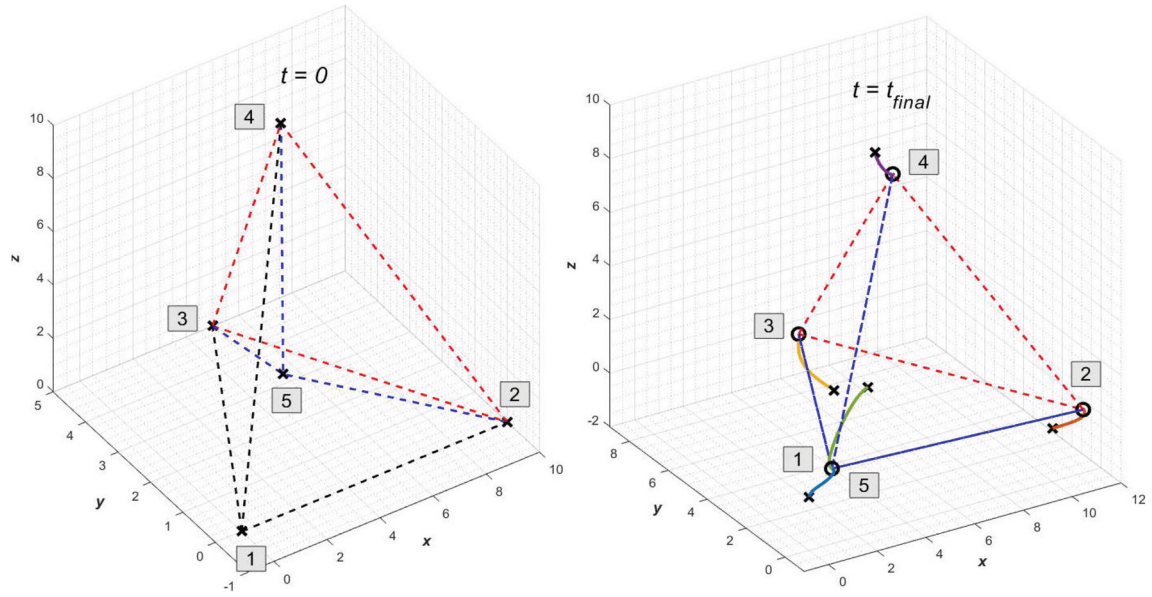

Fig. 5 Robot 5 initialized in the RoA to $F^*(\mathbf{q}^{*a})$ and *inside* of the tetrahedron formeded by robots 1-4. Crosses and circles denote initial and final positions, respectively. Robots 1 and 5 ocupy same final position due to convergence to the ambiguous formation

characterize on which side of the plane robot k is located. Finally, let r denote the distance from the centroid of the triangle formed by robots $k-3$, $k-2$, and $k-1$ to the farthest vertex of $F^*_{k-1}(\mathbf{q}^*_{k-1})$, as shown in Fig. 7. This parameter will be used to as a conservative estimate of the convex hull of the subformation. It is important to point out that r can be computed in advance for any desired subformation $F^*_{k-1}(\mathbf{q}^*_{k-1})$.

The control scheme described above is implementable through the control laws described next. For acquisition of subformations $F^*_k(\mathbf{q}^*_k)$, $k = 4, \ldots, N$, we use

$$u_i = -\alpha \sum_{j \in \mathcal{N}_i(\mathcal{E})} q_{ij} s_{ij}, \quad i = \mathcal{V} - \{k-2, k-1, k\}, \tag{13}$$

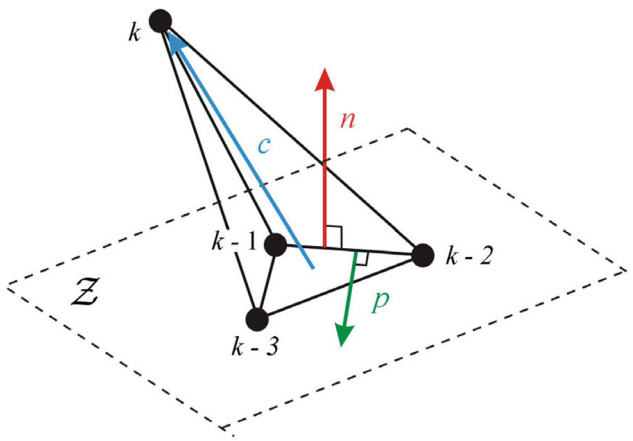

Fig. 6 Definition of vectors c, p, and n

$$u_i = \begin{cases} -\alpha \sum\limits_{j \in \mathcal{N}_i(\mathcal{E})} q_{ij} s_{ij}, & \text{if } c^\intercal \bar{n} < 0 \\ 0, & \text{if } c^\intercal \bar{n} \geq 0 \;\&\; \|c\| < r \\ \omega\left(p \times q_{(k-2)(k-1)}\right), & \text{if } c^\intercal \bar{n} \geq 0 \;\&\; \|c\| \geq r \end{cases}, \; i = \{k-2, k-1\} \tag{14}$$

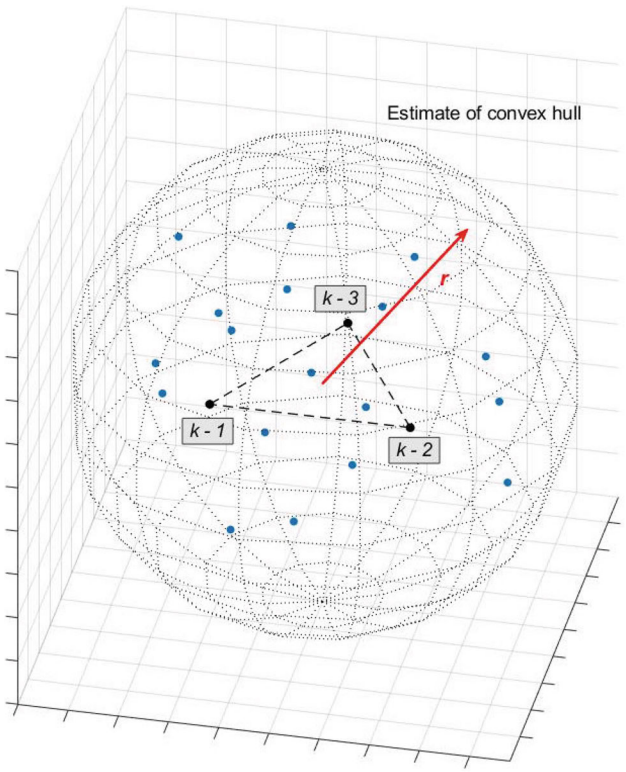

Fig. 7 Definition of parameter r. Points denote the desired subformation $F^*_{k-1}(\mathbf{q}^*_{k-1})$, and the sphere of radius r represents the convex hull estimate

and

$$u_k = \begin{cases} -\alpha \sum\limits_{j \in \mathcal{N}_k(\mathcal{E})} q_{kj} s_{kj}, & \text{if } c^\intercal \bar{n} < 0 \\ -\beta \dfrac{c}{\|c\|}, & \text{if } c^\intercal \bar{n} \geq 0 \ \& \ \|c\| < r \\ 0, & \text{if } c^\intercal \bar{n} \geq 0 \ \& \ \|c\| \geq r \end{cases} \quad (15)$$

where

$$\bar{n} = \begin{cases} n, & \text{if } q_k^* \text{ and } q_{k-4}^* \text{ on same side of plane } \mathcal{Z} \\ -n, & \text{if } q_k^* \text{ and } q_{k-4}^* \text{ on opposite sides of plane } \mathcal{Z}, \end{cases} \quad (16)$$

$\alpha, \beta > 0$ are control gains, ω is a user-defined constant denoting the angular speed of the rigid body rotation, and n was defined in Eq. (12).

Finally, to account for the situation where multiple robots are in their respective ambiguous RoA, we need to determine when subformation $F_l^*(\mathbf{q}_l^*)$ has been successfully acquired in order to initiate the acquisition of $F_m^*(\mathbf{q}_m^*)$ where $m > l \geq 4$. To this end, we utilize the error variables in Eq. (4) as indicators of successful subformation acquisition. Specifically, if

$$\max\left(\left|s_{l(l-1)}\right|, \left|s_{l(l-2)}\right|, \left|s_{l(l-3)}\right|\right) \leq \delta, \quad (17)$$

where δ is a sufficiently small, user-defined positive constant, then we consider that $F_l^*(\mathbf{q}_l^*)$ has been acquired and a signal is transmitted by robot l to robots $l+1$, $l+2$, and $l+3$. This signal is propagated through the graph using multi-hop routing until it reaches robot m.

Remark 1 Excluding robot 1, which always utilizes the conventional DBFC, a certain robot may use Eqs. (13), (14), or (15) depending on the subformation being acquired at the time.

Remark 2 Robots $k-3$, $k-2$, and $k-1$ play a distinctive function in the acquisition of subformation F_k. Specifically, the second rows in (14) and Eq. (15) correspond to robot k translating towards the triangle formed by robots $k-3$, $k-2$, and $k-1$ along the direction of vector $-c/\|c\|$ with linear speed β, while the third row corresponds to the rotation of robots $k-2$ and $k-1$ about vector p with angular speed ω. Since robots $1, \ldots, k-3$ use Eq. (13), they follow robots $k-2$ and $k-1$ and preserve the rigidity of subformation F_{k-1} for the duration of the event. Finally, the location of $\mathcal{R}(\mathbf{q}_k^*)$ relative to robot k is realized by the term $c^\intercal \bar{n}$ in Eqs. (14) and (15) whose sign indicates if $q_k(t) \in \mathcal{R}(\mathbf{q}_k^*)$ or $q_k(t) \in \mathcal{R}(\mathbf{q}_k^{*a})$ at any given time. The definition of $\bar{n}$ in Eq. (16) is solely for assuring that $c^\intercal \bar{n}$ is always negative whenever $q_k(t) \in \mathcal{R}(\mathbf{q}_k^*)$. Also, the conditions in Eq. (16) can be computed in advance since they depend on the desired formation only.

Remark 3 The above-described translation and rotation were selected because of their simplicity; i.e., they do not need path planning or additional information exchange between robots. Moreover, these maneuvers are free of collision. Observe that translation happens towards the centroid of the triangle formed by robots $k-3$, $k-2$, and $k-1$; thus, robot k will not collide with these robots when they are coplanar. Rotation happens when robot k is outside of rigid subformation F_{k-1}; thus, robots $1, \ldots, k-1$ will not collide with robot k.

Theorem 1 *Control system Eqs.* (13)-(15) *ensures that* $F(t) \to F^*(\mathbf{q}^*)$ *as* $t \to \infty$.

Proof It is well known that if the DBFC $u_i = \alpha \sum\limits_{j \in \mathcal{N}_i(\mathcal{E})} q_{ij} s_{ij}$ is used by *all* robots $i \in \mathcal{V}$ for *all* time, then $F(t) \to F^*(\mathbf{q}^*)$ or $F(t) \to F^*(\mathbf{q}^{*a})$ as $t \to \infty$ [4, 10]. Thus, when this control is applied to a subset of robots $i \in \bar{\mathcal{V}} \subset \mathcal{V}$ for all time, we have that $\|q_{ij}(t)\| \to d_{ij}$ (or equivalently $s_{ij}(t) \to 0$) as $t \to \infty$, $\forall (i,j) \in \mathcal{E}$ such that $i \in \bar{\mathcal{V}}$. When the distance-based control is applied to robots $i \in \bar{\mathcal{V}}$ for a *finite* time interval $[0, T]$, then $\left|s_{ij}(t)\right|$, $\forall (i,j) \in \mathcal{E}$ such that $i \in \bar{\mathcal{V}}$, are bounded and decreasing over $[0, T]$. Next, note that the control laws in the second and third rows of Eqs. (14) and (15) cause robots to move with finite velocity $\dot{q}_i$ since β and ω are constants. Since these control laws are only applied for a finite period of time until robot i reaches $\mathcal{R}(\mathbf{q}_i^*)$, the displacements experienced by the robots during this period will be bounded. As each robot $i = 4, \ldots, N$ sequentially reaches $\mathcal{R}(\mathbf{q}_i^*)$, its control system switches to the DBFC. Therefore, DBFC is applied to all robots $i \in \mathcal{V}$ after some finite period of time, after which no more switching occurs. As a result, $F(t) \to F^*(\mathbf{q}^*)$ as $t \to \infty$.

Remark 4 Since DBFC is a component of the proposed control system, known restrictions on the initial conditions associated with certain collocated, colinear, or coplanar situations still exist. However, the proposed control system enlarges the stability region since it does not require the robots to be initialized in the region of attraction to the desired formation, as is the case when using Eq. (7) by itself.

6 Simulation Results

The proposed formation control system was evaluated via a simulation conducted in MATLAB (version R2021a) script and compared to the 3D orthogonal basis formation controller of [14], which also has the ability to avoid flip ambiguities. We refer the reader to [14] for the details of the orthogonal basis control algorithm. The formation objective in the simulation consisted of six robots forming a 3D minimally rigid framework composed of three connected triangular pyramids as shown in Fig. 8. As such,

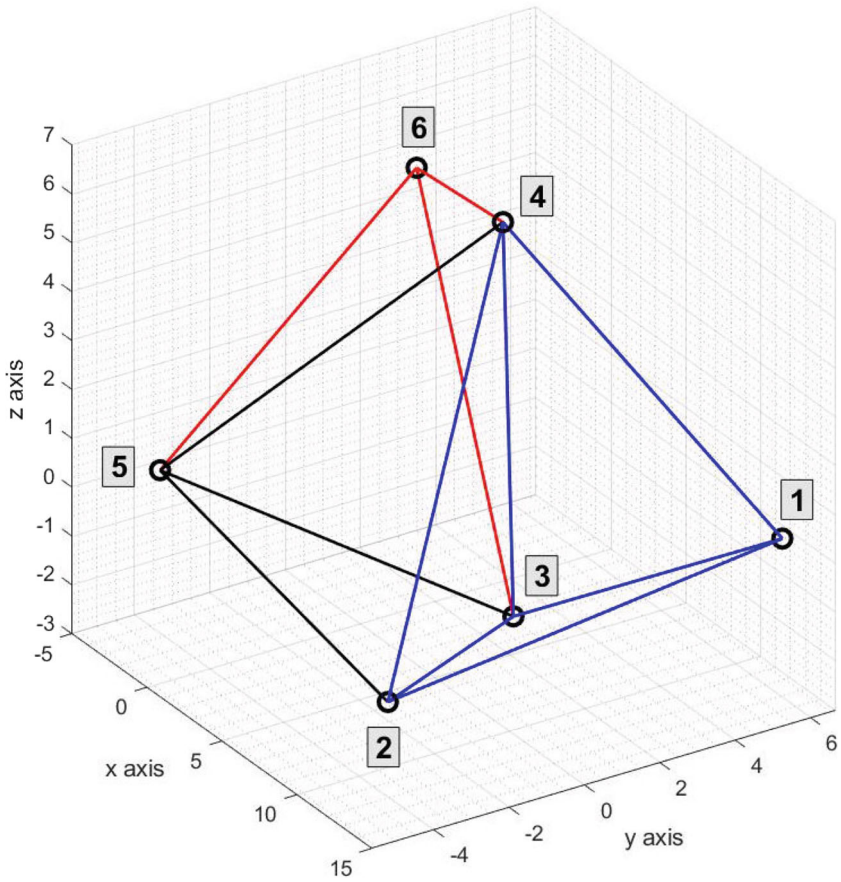

Fig. 8 Desired formation F^* composed of three triangular pyramids: first pyramid composed of vertices 1-4, second pyramid of vertices 2-5, and third pyramid of vertices 3-6

$N = 6$ and the edge set of size $3N - 6 = 12$ was $\mathcal{E} = \{(1,2), (1,3), (2,3), (1,4), (2,4), (3,4), (2,5), (3,5), (4,5), (3,6), (4,6), (5,6)\}$ where the desired distances were $d_{12} = d_{13} = d_{23} = d_{14} = d_{24} = d_{34} = d_{25} = d_{35} = d_{45} = d_{36} = d_{46} = d_{56} = 10$. For the chosen 3D shape, the desired distances between robots (1, 5) and (2, 6), although not explicitly controlled, would be equal to $20\sqrt{\frac{2}{3}}$. These distances are important because they indicate if flip ambiguities are avoided. In order to provide a proper basis for comparison of the two controllers, we imposed the control input constraint $\|u_i\| \leq 10, i = 1, \ldots 6$.

Two simulations were conducted for different initial conditions of the robots so that different switchings of Eqs. (14) and (15) occurred. The initial positions of the robots and the control gains of the switched controller for the two simulations are shown in Table 1. The orthogonal basis con-

Table 1 Simulation cases

	α	β	ω	Initial Position	
Simulation 1	0.01	10	10	$[-10, -10, -10]$	Robot 1
				$[10, 0, 0]$	Robot 2
				$[5, 5, 0]$	Robot 3
				$[5, 2.887, 10]$	Robot 4
				$[14, 16, 16]$	Robot 5
				$[7, 2, 4]$	Robot 6
Simulation 2	0.003	375	10	$[-100, -100, -100]$	Robot 1
				$[10, 0, 0]$	Robot 2
				$[5, 5, 0]$	Robot 3
				$[5, 2.887, 10]$	Robot 4
				$[-4, -6, -6]$	Robot 5
				$[-100, -107, -104]$	Robot 6

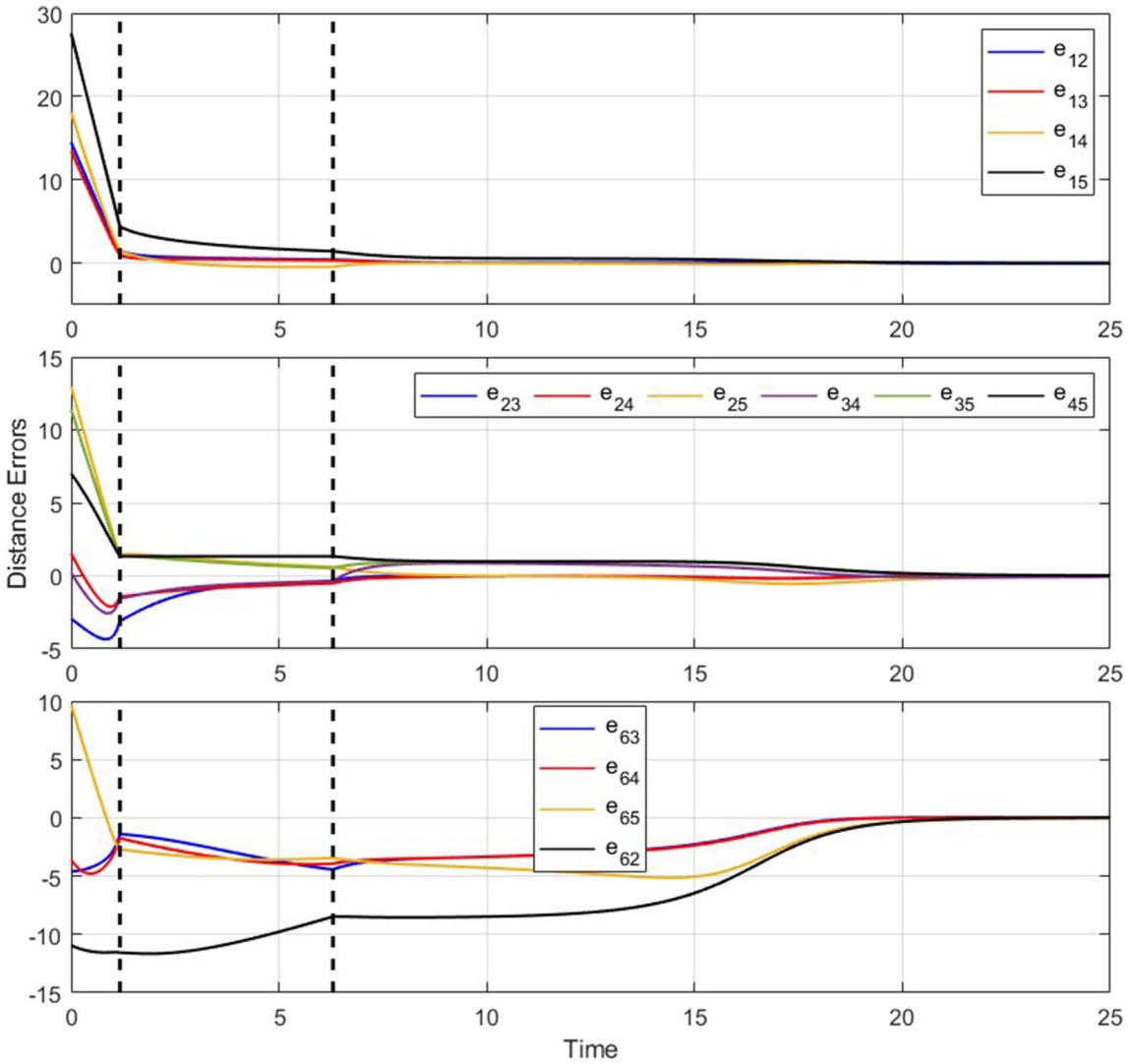

Fig. 9 Simulation 1: distance errors, e_{ij}, of the switched controller. Dashed vertical lines indicate switching instants

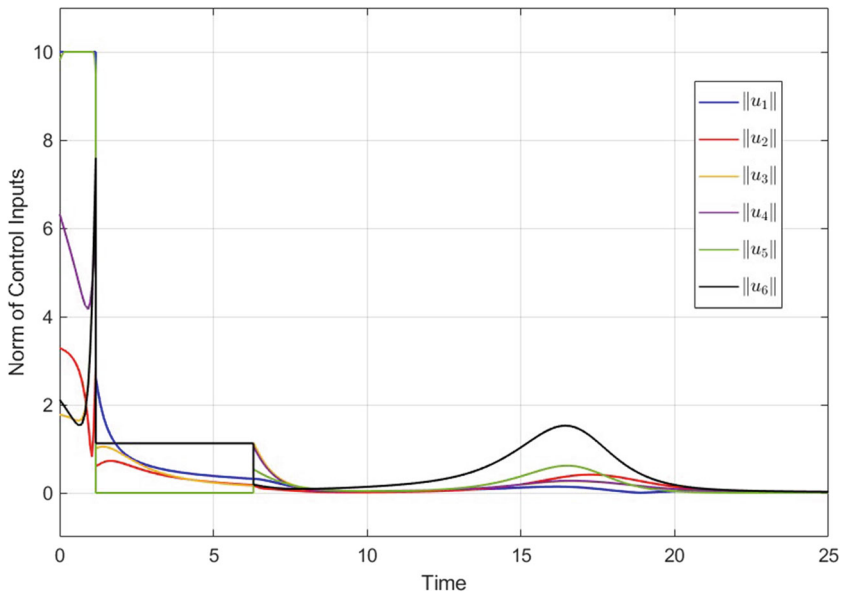

Fig. 10 Simulation 1: norm of the control inputs, $\|u_i\|$, of the switched controller

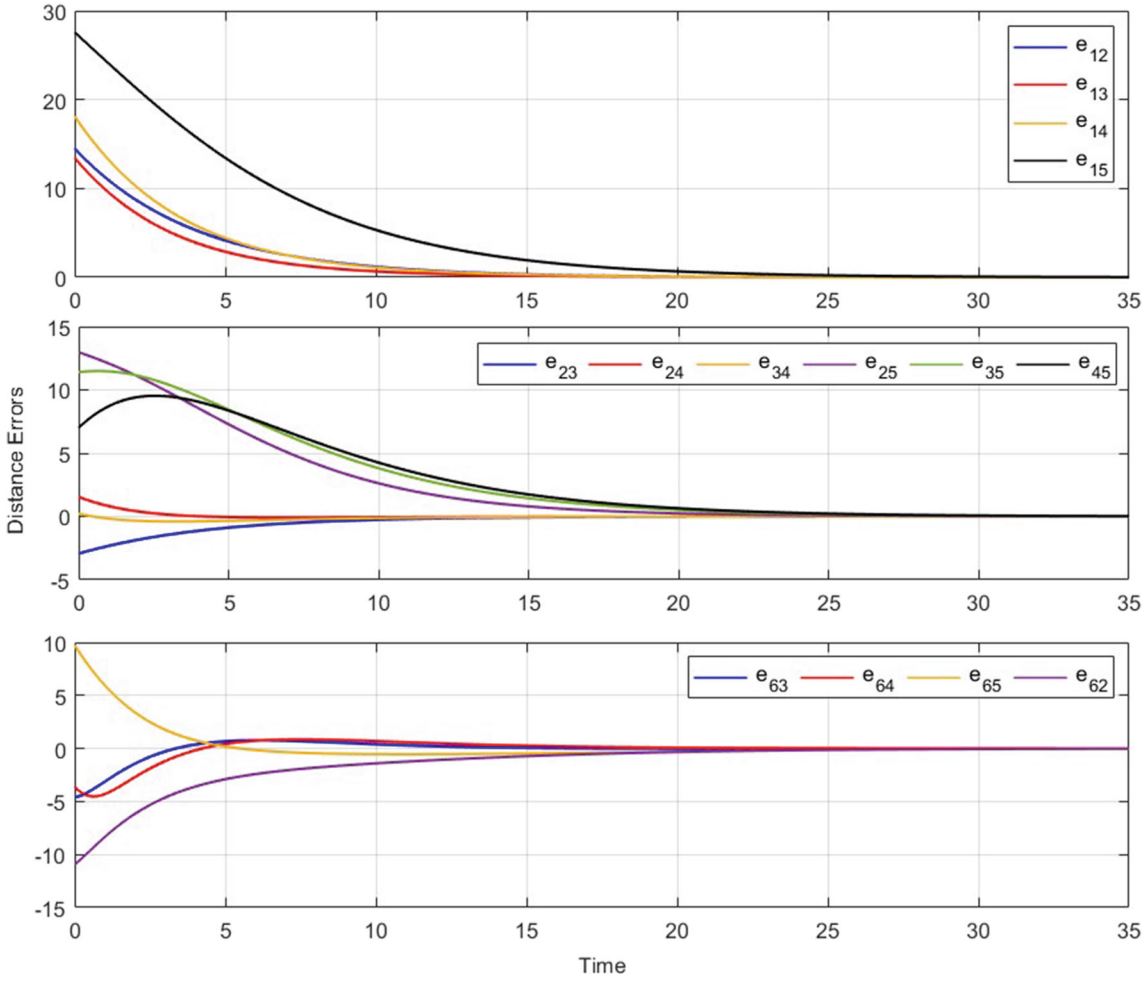

Fig. 11 Simulation 1: distance errors, e_{ij}, of the orthogonal basis controller

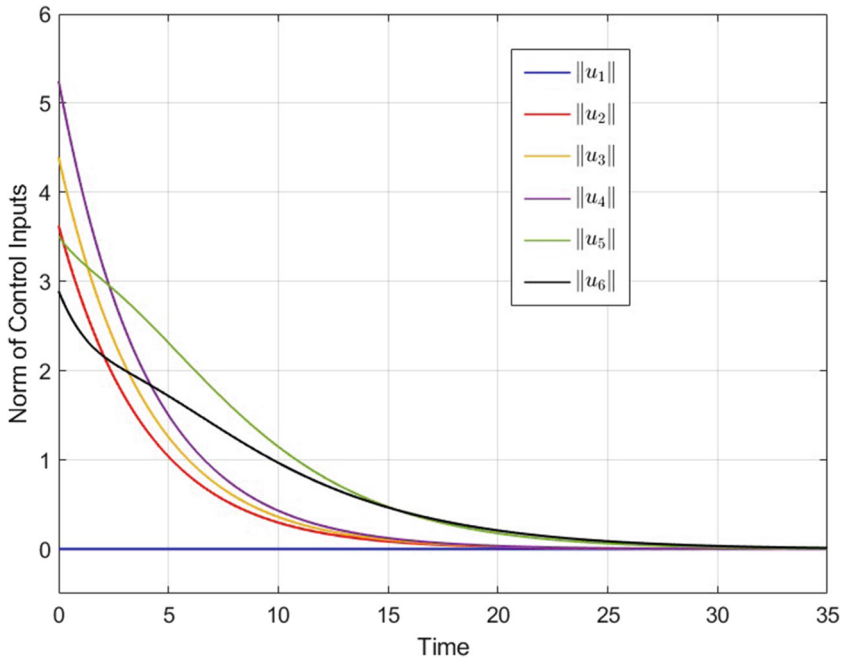

Fig. 12 Simulation 1: norm of the control inputs, $\|u_i\|$, of the orthogonal basis controller

Table 2 Comparison of Metrics

	T_s	E_c	Controller
Simulation 1	20.1	69.7	Switched
	25.7	106	Orthogonal Basis
Simulation 2	22.9	581	Switched
	41.6	861	Orthogonal Basis

troller was subjected to the same initial conditions and all its gains were set to 0.25 in both simulations (see [14] for the gain definitions). Two metrics were used to compare the performance of the switched and orthogonal basis controllers. First, if the actual, inter-robot distance errors are defined as $e_{ij}(t) = \|q_{ij}(t)\| - d_{ij}$, we computed the *settling time* T_s as the time for all distance errors to reach and remain within 2% of their corresponding desired distance, i.e., $|e_{ij}| \leq 0.02 d_{ij}$. Second, we computed the *control effort* as

$$E_c := \int_0^{T_s} \sum_{i=1}^{6} \|u_i(t)\| \, dt. \tag{18}$$

Animations of the simulations showing the 3D motion of the robots for each controller can be found in the YouTube playlist [20].

Simulation 1. The distance errors and norm of each control input for the proposed switched controller are shown in Figs. 9 and 10, respectively. For $t = [0, 1.17]$, the team of robots attempts to acquire F_4^* and F_5^* using Eq. (13), the first equation of Eqs. (14) and (15) with $k = 5$, and Eq. (17) with $\delta = 1.5$. At $t = 1.17$, Eq. (17) is met so the algorithm switches to address the fact that $q_6 \in \mathcal{R}(\mathbf{q}_6^{*a}) \cap \mathcal{C}(\mathbf{q}_5^*)$. This triggers the second equation in Eqs. (14) and (15) with $k = 6$

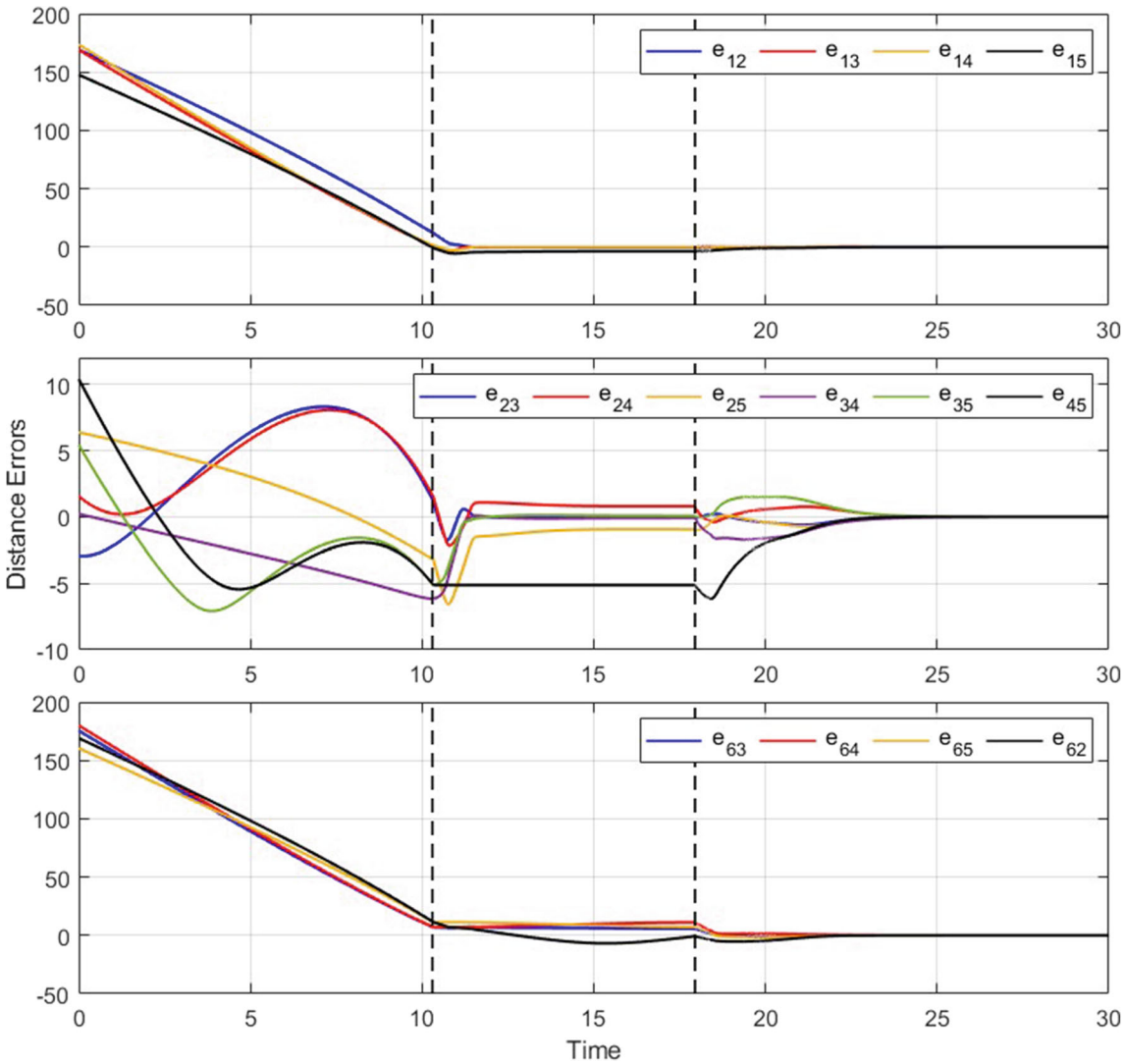

Fig. 13 Simulation 2: distance errors, e_{ij}, of the switched controller. Dashed vertical lines indicate switching instants

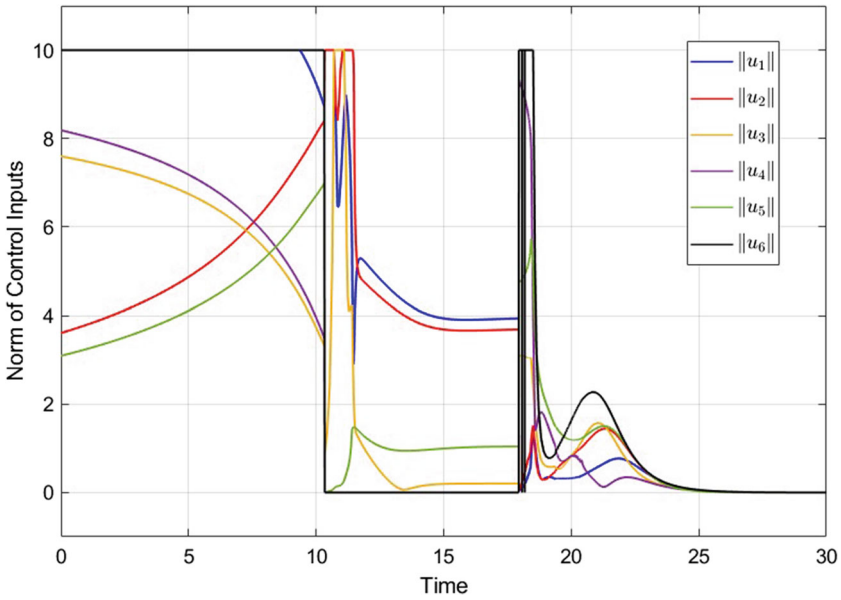

Fig. 14 Simulation 2: norm of the control inputs, $\|u_i\|$, of the switched controller

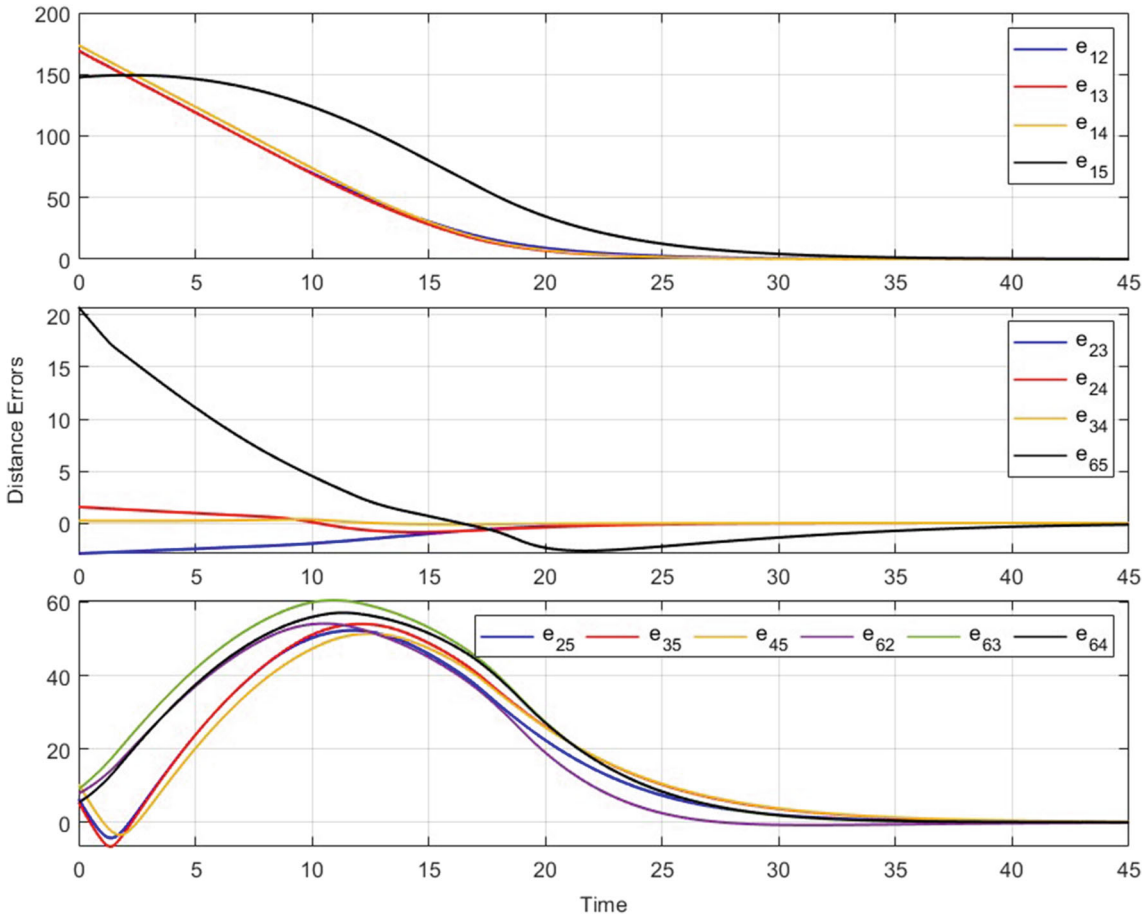

Fig. 15 Simulation 2: distance errors, e_{ij}, of the orthogonal basis controller

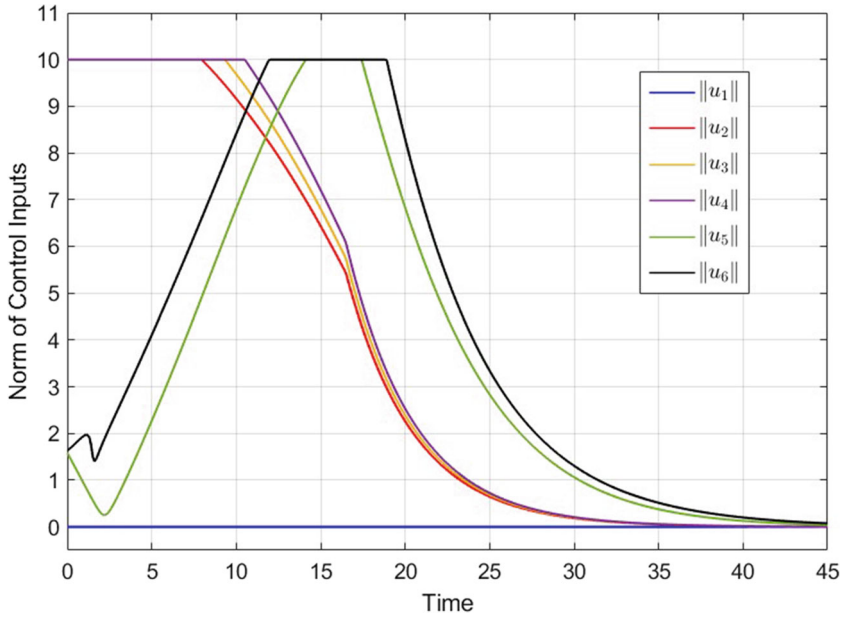

Fig. 16 Simulation 2: norm of the control inputs, $\|u_i\|$, of the orthogonal basis controller

and robot 6 *translates* towards the plane formed by robots 3-4-5. As seen from Fig. 10, the control inputs of robots 4 and 5 are zero during this period of time. At $t = 6.3$, $q_6 \in \mathcal{R}(\mathbf{q}_6^*)$ and the control systems for robots 4, 5, and 6 switch to the first equation in Eqs. (14) and (15) with $k = 6$. The desired formation is acquired by $t = 25$ as all distance errors are approximately zero; see Fig. 9. The distance errors and norm of the control inputs for the orthogonal basis controller are shown in Figs. 11 and 12, respectively. In this controller, robot 1 serves as the formation "anchor" since its control input is always zero. Notice that the desired formation takes longer to be acquired with the orthogonal basis controller. From Table 2, we can see that the switched controller outperforms the orthogonal basis control by having a shorter settling time with significantly less control effort.

Simulation 2. In this simulation, the initial conditions were such that robots 1 and 6 were positioned far from the rest of the robots at $t = 0$. The distance errors and control input norms of the switched controller are depicted in Figs. 13 and 14, respectively. Like in the first simulation, the robots prioritize the acquisition of F_4^* and F_5^* during the first 10.3 units of time. When Eq. (17) with $\delta = 1.5$ is met at $t = 10.3$, we have that $q_6 \in \mathcal{R}(\mathbf{q}_6^{*a}) \cap \bar{\mathcal{C}}(\mathbf{q}_5^*)$. This triggers the third equation in Eq. (14) and (15) with $k = 6$ and robots 4 and 5 begin rotating while robot 6 remains stationary. At $t = 18$, $q_6 \in \mathcal{R}(\mathbf{q}_6^*)$ so the control for robots 4, 5, and 6 switch to the first equation in Eqs. (14) and (15) with $k = 6$ and all robots operate with DBFC until the formation is successfully acquired at about $t = 23$. The results for the orthogonal basis controller are shown in Figs. 15 and 16. Again here, the switched control performs better by acquiring the desired formation faster and with less control effort.

7 Conclusion

In this paper, we introduced a switched control system for preventing flip ambiguities in distance-based 3D formation problems. The novelty of the proposed approach was bypassing added variables, e.g. the signed volume, in the formation controller. The control system was devised for 3D Henneberg frameworks where each robot has control, sensing, and communication channels with the previous three robots in the vertex set, resulting in a tetrahedralized, minimally rigid graph. The control scheme maneuvers the formation away from the region of attraction to the flip ambiguity and then switches to the conventional distance-based formation controller. As a result, the control ensures formation shape acquisition for a larger set of initial conditions. The proposed control strategy is agnostic to the type of mobile robot since it is based on a high-level motion model defined by the single-integrator equation. In practice, our control can be embedded in a low-level control loop that accounts for the robot dynamics.

Author Contributions FS and MdQ co-designed the control strategy and co-wrote the manuscript. FS conducted the simulations.

Funding The research leading to these results received funding from NASA under grant number NNX15AH82H.

Declarations

Competing of interest The authors have no relevant financial or non-financial interests to disclose.

References

1. Anderson, B.D.O., Yu, C., Fidan, B., Hendrickx, J.M.: Rigid graph control architectures for autonomous formations. IEEE Contr. Syst. Mag. **28**(6), 48–63 (2008)
2. Anderson, B.D.O., Sun, Z., Sugie, T., Azuma, S., Sakurama, K.: Formation shape control with distance and area constraints. IFAC J. Syst. Control **1**, 2–12 (2017)
3. Cao, Y., Sun, Z., Anderson, B. and Sugie, T. (2019) Almost global convergence for distance-and area constrained hierarchical formations without reflection. In: Proc. IEEE Intl. Conf. Control Autom., pp. 1534–1539
4. de Queiroz, M., Cai, X., Feemster, M.: Formation control of multi-agent systems: A graph rigidity approach. Wiley, Hoboken, NJ (2019)
5. Ferreira-Vazquez, E.D., Hernandez-Martinez, E.G., Flores-Godoy, J.J., Fernandez-Anaya, G., Paniagua-Contro, P.: Distance-based formation control using angular information between robots. J. Intell. & Robotic Syst. **83**(3–4), 543–560 (2016)
6. Ferreira-Vazquez, E.D., Flores-Godoy, J.J., Hernandez-Martinez, E.G., and Fernandez-Anaya, G. (2016) Adaptive control of distance-based spatial formations with planar and volume restrictions. In: Proc. IEEE Conf. Control Appl., pp. 905–910, Buenos Aires, Argentina
7. Grasegger, G., Koutschan, C., Tsigaridas, E.: Lower bounds on the number of realizations of rigid graphs. Experim. Math. **29**(2), 125–136 (2020)
8. Izmestiev, I.: Infinitesimal Rigidity of Frameworks and Surfaces. Kyushu University, Japan, Lectures on Infinitesimal Rigidity (2009)
9. Jackson, B. (2007) Notes on the Rigidity of Graphs. Notes of the Levico Conference, Levico Terme, Italy
10. Krick, L., Broucke, M.E., Francis, B.A.: Stabilisation of infinitesimally rigid formations of multi-robot networks. Intl. J. Control **82**(3), 423–439 (2009)
11. Liu, T., de Queiroz, M., Zhang, P., Khaledyan, M.: Further results on the distance and area control of planar formations. Intl. J. Control **94**(3), 767–783 (2021)
12. Liu, T., de Queiroz, M.: Distance + angle-based control of 2d rigid formations. IEEE Trans. Cybern. **51**(12), 5969–5978 (2021)
13. Liu, T., de Queiroz, M. and Sahebsara, F. (2020) Distance-based planar formation control using orthogonal variables. In: Proc. IEEE Conf. Control Techn. Appl., pp. 64–69, Montreal, Canada
14. Liu, T., de Queiroz, M.: An orthogonal basis approach to formation shape control. Automatica **129**, 109619 (2021)
15. Mesbahi, M., Egerstedt, M.: Graph theoretic Methods in Multiagent Networks. Princeton University Press, Princeton, NJ (2010)
16. Oh, K.-K., Park, M.-C., Ahn, H.-S.: A survey of multi-agent formation control. Automatica **53**, 424–440 (2015)
17. Park, M., Kim, H. and Ahn, H. (2017) Rigidity of distance-based formations with additional subtended-angle constraints. In:Proc. Intl. Conf. Control, Autom., and Syst., pp. 111–116, Jeju, Korea
18. Sahebsara F. and de Queiroz, M. (2021) Avoiding flip ambiguities during sequentially-grown formations. In:Proc. AACC Modeling, Estimation and Control Conf., pp. 657–662, Austin, TX
19. Sugie, T., Anderson, B.D., Sun, Z. and Dong, H. (2018) On a hierarchical control strategy for multi-agent formation without reflection. In:Proc. IEEE Conf. Dec. Control, pp. 2023–2028, Miami Beach, FL
20. Simulation Animations (2023) https://www.youtube.com/playlist?list=PLKXaQfLd5M55rOQZP8BD95dh2WjyD4UC6

Farid Sahebsara received a B.S. Degree in Mechanical Engineering from K. N. Toosi University of Technology, Iran and an M.S. Degree in Mechanical Engineering from Amirkabir University of Technology (Tehran Polytechnic), Iran. He is currently pursuing a Ph.D. in Mechanical Engineering at Louisiana State University, where he serves as a graduate research assistant. His research focuses on multi-agent systems, robotics, and multi-body dynamics.

Marcio de Queiroz received a B.S. Degree in Electrical Engineering from the Federal University of Rio de Janeiro, Brazil, a M.S. Degree in Mechanical Engineering from the Pontifical Catholic University of Rio de Janeiro, Brazil, and a Ph.D. Degree in Electrical Engineering from Clemson University, Clemson, SC in 1997. From August 1997 to August 1998, he was a Post-Doctoral Researcher at the Rotating Machinery and Controls Laboratories of the University of Virginia. From September 1998 to May 2000, he was a Visiting Assistant Professor at the Department of Mechanical Engineering of the NYU Tandon School of Engineering. In July 2000, he joined the Department of Mechanical and Industrial Engineering at LSU, where he is currently the Roy O. Martin Lumber Company Professor. In 2005, he was the recipient of the NSF CAREER award. Dr. Queiroz served as an Associate Editor for the IEEE Transactions on Automatic Control, the ASME Journal of Dynamic Systems, Measurement, and Control, the IEEE/ASME Transactions on Mechatronics, and the IEEE Transactions on Systems, Man, and Cybernetics – Part B. He is currently the coordinator for the Robotics Engineering minor for the LSU College of Engineering. His research interests include nonlinear control theory and applications, multi-agent systems, robotics, active magnetic and mechanical bearings, and biological/biomedical system modeling and control. Dr. Queiroz is a Fellow of the American Society of Mechanical Engineers.